Biochemistry

Subscriber access provided by MIDWESTERN UNIVERSITY

Article

Antioxidative pseudo-enzymatic mechanism of NAD(P)H coexisting with oxyhemoglobin for suppressed methemoglobin formation

Magohei Yamada, Takashi Matsuhira, Keizo Yamamoto, and Hiromi Sakai

Biochemistry, **Just Accepted Manuscript** • DOI: 10.1021/acs.biochem.8b01314 • Publication Date (Web): 21 Feb 2019

ACS Publications

is published by the American Chemical Society. 1155 Sixteenth Street N.W., Washington, DC 20036

Revised manuscript submitted to *Biochemistry*

ID: bi-2018-013145-R1

Antioxidative pseudo-enzymatic mechanism of NAD(P)H coexisting with oxyhemoglobin for suppressed methemoglobin formation

Magohei Yamada, Takashi Matsuhira, Keizo Yamamoto, and Hiromi Sakai*

Department of Chemistry, Nara Medical University

840 Shijo-cho, Kashihara, Nara 634-8521, Japan

* To whom correspondence should be addressed:

Prof. Hiromi Sakai, Department of Chemistry, Nara Medical University

840 Shijo-cho, Kashihara, Nara 634-8521, Japan

Tel. and Fax: +81-744-29-8810; E-mail: hirosakai@naramed-u.ac.jp

Abstract

Oxyhemoglobin (HbO_2) coexisting with equimolar NADH retards autoxidation and oxidants-induced metHb formation based on the pseudo-catalase (CAT) and pseudo-superoxide dismutase (SOD) activities. In this work we compared the effects of NADH with those of NADPH and estimated the binding site of NAD(P)H to HbO_2 to elucidate the antioxidative mechanisms. Results clarified that pseudo-CAT and pseudo-SOD activities of HbO_2 coexisting with NADPH were similar to activities obtained with NADH. Prompt MetHb formation (< 40 min) facilitated by oxidants (H_2O_2, NO, $NaNO_2$) was hindered by NADPH. These effects were similar to those of NADH. However, we found that NADPH is thermally unstable compared to NADH, and that NADPH cannot sustain antioxidative effects for a long period of autoxidation to metHb such as 24 h. Lineweaver–Burk plots clarified that the Michaelis constants of these pseudo-enzymatic activities are of millimolar order. Addition of inositol hexaphosphate (IHP) and 2,3-diphosphoglycerate (DPG), which are known to bind not only with deoxyHb but also weakly with HbO_2, showed competitive inhibition of pseudo-enzymatic activities. These results suggest that the binding site of NADH and NADPH on HbO_2 is the same as those of IHP and DPG. ^{31}P NMR surely clarified 1:1 stoichiometric NADH binding to HbO_2. HPLC analysis showed that NADH preferentially inhibited autoxidation of α-subunit heme. Docking simulations predicted that the binding site of the relax-state HbO_2 with NAD(P)H is equal to those with IHP and DPG. Collectively, the pseudo-enzymatic activities of HbO_2 coexisting with NAD(P)H is induced by the 1:1 stoichiometric binding of NAD(P)H to HbO_2.

(250 words)

INTRODUCTION

Ferrous oxyhemoglobin (HbO_2) gradually autoxidizes to form ferric methemoglobin (metHb) that cannot bind oxygen.[1,2] During this process, superoxide anion ($O_2^{\cdot -}$) is released ($HbO_2 \rightarrow metHb + O_2^{\cdot -}$), forming hydrogen peroxide[3] via a disproportionation reaction, enhancing further oxidation of HbO_2 and deoxyHb to converting them to metHb. In addition to these reactive oxygen species (ROS), reactive nitrogen species (RNS) such as nitric oxide (NO) and nitrite (NO_2^-) present in the blood contribute to conversion of Hb to metHb.[4] Red blood cells (RBCs) have various functions to reduce metHb and contain catalase (CAT) and superoxide dismutase (SOD) decomposing ROS. Ferric metHb is reduced enzymatically to a ferrous state by the action of NADH-cytochrome b_5 reductase, which requires a substrate of reduced form of nicotinamide adenine dinucleotide (NADH) as well as cytochrome b_5 as an intermediate electron mediator.[5] Nicotinamide adenine dinucleotide phosphate (NADPH)-metHb reductase and NADPH-flavin reductase, which require a coenzyme of NADPH, reduce metHb.[6] The oxidized form $NADP^+$ is reduced to NADPH[7] via the pentose phosphate pathway.

Our earlier report described that the coexistence of equimolar amount of NADH with HbO_2, with no corresponding enzymes described above, retarded autoxidation of HbO_2 for 24 h in a physiological condition (37 °C, pH 7.4).[8] However, the similar molecule of NADPH did not inhibit metHb formation. We reported that NADH coexisting with HbO_2 showed pseudo-CAT and pseudo-SOD activities.[8] By trying co-encapsulation of NADH to artificial red blood cells (liposome-encapsulated Hbs), we found that autoxidation of the artificial red blood cells was inhibited in a rat model. In that experiment, the intra-liposomal NADH concentration was 1.5 mM: approximately 100 times greater than that in a human RBC (NAD^+, 0.065 mM; NADH,

0.00028 mM; 0.06528 mM in total).[9] Actually, NADH is useful with artificial red blood cells for clinical use because the safety of NADH is proven.[10]

Our earlier study produced no detailed explanation of the mechanism of the pseudo-enzymatic activities.[8] Although NADPH is quite similar to NADH in terms of its structure and standard redox potential, NADPH showed inferior inhibition effects on autoxidation of HbO_2. As described in this paper, we first investigated their pseudo-CAT and pseudo-SOD activities of NAD(P)H coexisting with HbO_2, their inhibitory effects on metHb formation induced by the addition of oxidants (H_2O_2, NO, and $NaNO_2$), and their thermal stability to clarify reasons for similarities and differences between NADH and NADPH. Secondly, we strove to clarify the mechanism of inhibition effects of metHb formation from the perspective of binding interaction between HbO_2 and NAD(P)H. The Michaelis constant of each pseudo-enzymatic activity was determined. Inositol hexaphosphate (IHP) and 2,3-diphosphoglycerate (DPG) are known to bind weakly to HbO_2 in a relaxed state.[11,12] Profiles of the inhibition effect of IHP and DPG were investigated. ^{31}P NMR and docking simulations were conducted for the investigation of binding sites of NAD(P)H on HbO_2. The results provide insight and information related to the antioxidative pseudo-enzymatic mechanism of NAD(P)H coexisting with HbO_2.

MATERIALS AND METHODS

Purification of Hb from Red Blood Cells—Experiments using human-derived Hb were approved by the ethical committee of Nara Medical University. Hb (a main component, adult human hemoglobin) was purified from RBCs as described in earlier reports.[13,14] One Hb is consisted of two alpha subunits and two beta subunits. UniProtKB entry P69905 is for hemoglobin subunit alpha, and entry P68871 is for beta. Outdated packed RBCs were provided by the Japanese Red Cross Society. Purified HbO_2 solution was obtained via carbonylation, pasteurization, nanofiltration, dialysis, and decarbonylation.[8] Absence of residual enzymatic activities in the HbO_2 solution was confirmed. MetHb was prepared using a method described in an earlier report.[8,15]

MetHb Formation Induced by Oxidants and Inhibitory Effect of NAD(P)H—NADH and NADPH were purchased from Oriental Yeast Co., Ltd. and Sigma-Aldrich Corp., respectively. Three oxidants that promote metHb formation were used: (1) 1-hydroxy-2-oxo-3-(*N*-methyl-3-aminopropyl)-3-methyl-1-triazene (NOC7; Dojindo Molecular Technologies Inc.), (2) $NaNO_2$ (Wako Pure Chemical Industries Ltd.), and (3) 30 wt% H_2O_2 (Wako Pure Chemical Industries Ltd.). The HbO_2 solution (30 μL, 10.1 g/dL) was diluted with 3 mL of PBS (pH 7.4; Gibco Life Technologies Co.) (final Hb concentration, 100 mg/dL, 15.6 μM). Then it was incubated with each of the oxidants at the molar equivalent to that of HbO_2 at 37 °C. The metHb-specific absorbance at 630 nm was measured to evaluate the effects of equimolar NAD(P)H on metHb formation.

Thermal Stability Evaluation of NAD(P)H—NADPH and NADH (1.6 mM) were

dissolved in PBS (pH 7.4). Then 10 mL of the solution was sealed in glass vials. Each vial was incubated either for 7 days at 25 °C, 3 days at 30 °C, 2 days at 37 °C, or 3 h at 50 °C. During the incubation NAD(P)H was oxidized by the dissolved dioxygen to form $NAD(P)^+$. The change of the concentration of the reduced form was monitored by the absorbance at 340 nm using a spectrophotometer (V-660; Jasco Corp.) equipped with an integral sphere unit (ISV-722). After each incubation condition, the percentage of the remaining reduced form (recovery) was calculated from the decrease in the absorption at 340 nm. The time necessary to decrease to 80% recovery ($t_{0.8}$) and 20% recovery ($t_{0.2}$) were calculated. Rate constant (k) for the oxidation of NAD(P)H was calculated for each incubation condition. Graphs of Arrhenius plots were made to obtain the activation energy (E_a).

Pseudo-enzymatic Activities of NADPH–Hb Mixed System—Pseudo-CAT and pseudo-SOD activity values were measured using a method reported earlier.[8] (1) CAT activity was measured in 1000-times diluted Hb solution based on the change in 230 nm absorbance of H_2O_2.[16] (2) SOD activity was measured in 100-times diluted Hb solution using pyrogallol autoxidation method.[17,18] Pyrogallol (Wako Pure Chemical Industries Ltd.) autoxidizes and thereby generates superoxide. Then the solution becomes yellow with 420 nm absorbance. This reaction is inhibited by the presence of SOD. The SOD activity was measured based on the inhibitory effect. The analytes included purified HbO_2, HbCO, and metHb solutions with or without NADPH. The results were compared with previously reported values of NADH-Hb mixed system and stroma-free hemolysates (SFHL) containing native SOD and CAT prepared from blood of three individuals.

Kinetic Parameters of the Pseudo-enzymatic Activities and Influence of IHP and

DPG—Lineweaver–Burk plots were made by plotting the inversed pseudo-enzymatic activities ($1/V$) and the inversed concentration of NAD(P)H ([HbO_2] = 1.5 mM, [NAD(P)H] = 1–15 mM). The maximum enzymatic activity (V_{max}) and the Michaelis constant (K_m) were calculated from the graphs. IHP and DPG were selected as potential inhibitors for pseudo-enzymatic activities because they are known to bind HbO_2. Both IHP and DPG were purchased from Sigma-Aldrich Corp. The concentration of the potential inhibitor was equal to NAD(P)H. The values of V_{max}, K_m and the inhibition dissociation constant (K_i) were calculated from Lineweaver–Burk plot data.

Influences of the Addition of NAD$^+$, NADP$^+$, and PLP—For detailed insight into the mechanisms, the oxidized forms of NAD(P)H, NAD^+ and $NADP^+$, were tested to ascertain whether they show inhibitory effects. Pyridoxal 5'-phosphate (PLP) was also tested for the potential inhibitor because PLP is known to bind to Hb as an allosteric effector. NAD^+ and PLP were purchased from Sigma-Aldrich Corp.; $NADP^+$ was from Oriental Yeast Co. Ltd. (Tokyo, Japan). Lineweaver–Burk plots were made by plotting the inversed pseudo-enzymatic activities and the inversed concentration of NAD(P)H in the presence of equimolar NAD^+, $NADP^+$, or PLP.

HPLC Analyses of the Autoxidation Intermediate Hybrids of HbO_2 in the Presence of NADH—The HbO_2 solutions (1.5 mM) in PBS in the presence and absence of 1.5 mM NADH were incubated at 37 °C. Aliquots of the solutions were periodically pipetted out and analyzed by HPLC (Chromaster; Hitachi High-Technologies Corp., Tokyo, Japan) equipped with an ion-exchanging column, TSKgel SP-NPR (Tosoh Corp, Tokyo, Japan). An analyte solution was injected into the column through a sampler. Intact HbO_2 ($\alpha_2\beta_2$), partially oxidized intermediate hybrids ($\alpha_2\beta_2^+$, $\alpha_2^+\beta_2$), and totally oxidized metHb ($\alpha_2^+\beta_2^+$) were separated by the column using a

5 min linear gradient from 0.05 to 0.2 M sodium chloride in 20 mM bis-Tris-HCl buffer (pH 6.0) at a flow-rate of 1.5 mL/min. Effluent was monitored using a diode array detector (5430 Diode Array Detector; Hitachi High-Technologies Corp.) with absorbance at 411 nm, which corresponds to the isosbestic point of metHb and HbO_2. The assignments of the two intermediate hybrid signals, $\alpha_2\beta_2^+$ and $\alpha_2^+\beta_2$, and the totally oxidized $\alpha_2^+\beta_2^+$ were taken from Tomoda et al.[27]

^{31}P NMR of NADH in the Presence of HbO_2—The ^{31}P-NMR with ^{1}H decoupling spectra of NADH were obtained on the JEOL JNM-ECZ500R (JEOL RESONANCE Co., Tokyo, Japan), equipped with a 5 mm ROYAL probe, at 202.27 MHz. Chemical shifts were referenced to 85% H_3PO_4 (0 ppm). The spectra were the results of accumulating 512 scans at 25.3 °C, with 32k data points, at a 45° pulse angle, 4 s relaxation delay, and 5.29 s repetition time. The analyte solutions of NADH (1.5 mM) in PBS in the presence of HbO_2 (0, 0.5, 1.0, and 1.5 mM) were measured. The assignments of the chemical shifts were taken from the references.[19-21] From the integrated intensities of the signals, the ratio of the amount of NADH being interacted with HbO_2 was calculated for all the analytes. We did not measure NADHP because of its instability that might cause decomposition during the preparation of the analyte solutions and a long-term NMR analysis.

Docking Simulation of NAD(P)H and Hb—All docking simulations were performed using the MF myPresto v3.2 mmMPApp2 applications (FiatLux Co. Ltd., Tokyo, Japan). The PDB files of the registered structure were converted into files for MF myPessto. The PDB files used were HbO_2 (PDB code, 1HHO[22]), deoxyHb (2HHB[23]), NADH (2JHF[24]), and NADPH (1US0[25]). Topology “Tplgene” data were made for “protein” (HbO_2 or deoxyHb) and “ligand” (NAD(P)H) for docking simulation. After the docking simulation, the main interatomic distances

were measured using WebLab Viewer Lite – Molecular Visualization Software (WLViewerLite 40) with the data of the docking simulation. The figures of the binding sites were described using the PyMOL Molecular Graphic System (Ver. 1.6, Schrödinger, LLC, New York).

RESULTS

MetHb Formation in HbO_2 Solution by the Addition of Oxidants and Inhibitory Effects of NADPH—According to our earlier study,[8] HbO_2 solution was purified via carbonylation, pasteurization, nanofiltration, and decarboxylation. In the HbO_2 solution, no other protein was detected using high performance liquid chromatography, sodium dodecyl sulfate polyacrylamide gel electrophoresis, or isoelectric focusing. Furthermore, no enzymatic activity of SOD, CAT, NADH-metHb reductase, or NADPH-diaphorase was found, indicating complete elimination of enzymes during purification.[8] All experiments described below used this purified HbO_2 solution.

The effects of addition of oxidants including H_2O_2, $NaNO_2$, and NO to an HbO_2 solution were evaluated. For NO production, 1-hydroxy-2-oxo-3-(*N*-methyl-3-aminopropyl)-3-methyl-1-triazene (NOC7) was used. It discomposes in aqueous solution generating NO. The addition of oxidants induced metHb formation. HbO_2 was oxidized almost completely in 40 min (**Figure 1**). By contrast, the coexistence of NADPH and NADH caused clear retardation of metHb formation. In the HbO_2 solution with equivalent molar of NADPH, the levels of metHb after 40 min incubation with H_2O_2, $NaNO_2$, and NOC7 were 58%, 47%, and 63%, respectively of the levels obtained in cases without NADPH. In fact, NADH showed 5–8% lower levels of metHb than NADPH did, but the inhibitory effects were similar.

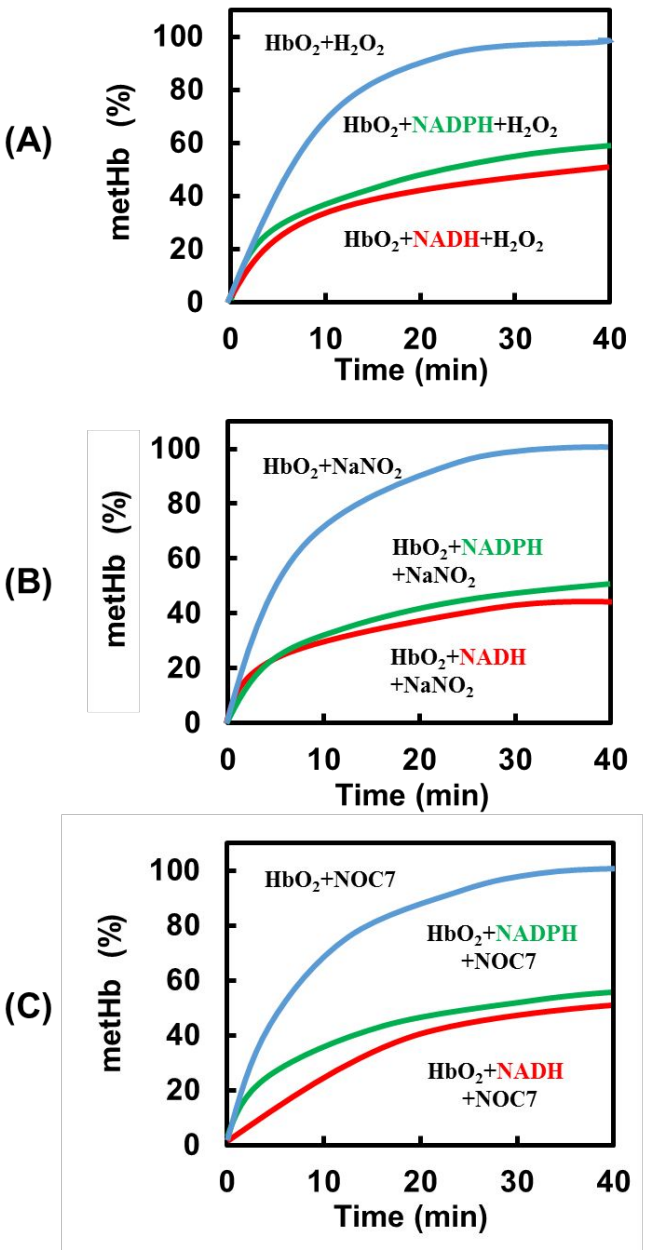

Figure 1. Time course of metHb level (%) of HbO_2 solution with and without NADPH (or NADH) after the addition of oxidants: (A) H_2O_2, (B) $NaNO_2$, and (c) NOC7. The initial concentrations of HbO_2, NADPH (or NADH), $NaNO_2$, H_2O_2, and NOC7 were all 15.6 μM in the cuvettes. The concentration of metHb (%) was calculated based on the increase of absorbance at 630 nm. The absorbance changes of Hb without NADPH (or NADH) after incubation at 25 °C for 40 min were defined as 100%.

Measurement of Pseudo-Enzymatic Activities of NADPH and Hb Solution Mixed System—**Table 1** presents pseudo-enzymatic activities (CAT and SOD) of NAD(P)H coexisting with Hb. Data for NADH reported previously[8] were inserted for comparison. Pseudo-enzymatic activities for NADPH coexisting with HbO_2 showed similar levels to those compared with those for NADH (Entries No. 1–5). Combination with HbO_2 showed higher activities compared to those with metHb and HbCO (Entries No. 6–7). NADPH alone showed pseudo-activity, as did NADH, based on the measurement principles (Entries No. 8–11), but they were much lower than those of the mixture of NADPH and HbO_2. Because both NADH and NADPH are known to react with H_2O_2,[26] increasing their concentrations showed higher pseudo-CAT activities based on the measurement principles. The pseudo-SOD activities were low. Moreover, there was apparently no concentration dependence. NAD(P)H coexisting with HbO_2 showed comparable enzymatic activities with those of stroma-free hemolysate (SFHL) containing native enzymes (Entry No. 12).

Table 1. Pseudo-catalase (CAT) and pseudo-superoxide dismutase (SOD) activities in Hb solution with or without coexistence of NADPH (and NADH as a reference[8]) [a]

Entry No.	State of Hb	Hb (mM)	Potential Antioxidant	Potential Antioxidant concentration (mM)	Pseudo-CAT ($\times 10^4$IU/g Hb)	Pseudo-SOD ($\times 10^2$ U/g Hb)
1	HbO_2	1.5	NADPH	0.5	5.2±1.1	1.5±1.4
			(NADH)	(0.5)	(6.2±1.7)	(2.1±1.7)
2	HbO_2	1.5	NADPH	1.0	17.6±2.1	6.7±2.1
			(NADH)	(1.0)	(19.2±1.4)	(7.6±1.5)
3	HbO_2	1.5	NADPH	1.5	23.6±1.6	12.6±1.0
			(NADH)	(1.5)	(34.3±1.2)	(15.6±0.9)
4	HbO_2	1.5	NADPH	3.0	26.8±0.8	14.8±1.8
			(NADH)	(3.0)	(35.2±1.0)	(16.0±1.2)
5	HbO_2	1.5	NADPH	15.0	36.0±2.1	16.3±0.8
			(NADH)	(15.0)	(46.8±1.2)	(20.4±1.4)
6	metHb	1.5	NADPH	1.5	4.2±1.0	1.3±0.4
			(NADH)	(1.5)	(4.5±1.4)	(1.2±0.6)
7	HbCO	1.5	NADPH	1.5	0.5±0.3	1.0±0.6
			(NADH)	(1.5)	(0.5±0.4)	(1.0±0.5)
8	-	-	NADPH	1.5	3.4±0.6[b]	1.1±0.7[b]
			(NADH)	(1.5)	(3.6±0.4)[b]	(1.1±0.7)[b]
9	-	-	NADPH	3.0	3.9±0.7[b]	1.2±0.7[b]
			(NADH)	(3.0)	(4.1±0.8)[b]	(1.3±1.6)[b]
10	-	-	NADPH	30.0	20.2±0.9[b]	1.0±0.6[b]
			(NADH)	(30.0)	(19.2±0.6)[b]	(0.6±0.6)[b]
11	-	-	NADPH	45.0	20.6±0.6[b]	1.7±0.7[b]
			(NADH)	(45.0)	(19.9±0.8)[b]	(1.6±0.5)[b]
12	HbO_2	1.5	-	-	N.D.[d]	N.D.[d]
13	SFHL (HbO_2)[c]	1.5	-	-	20.1±1.4	21.6±1.7

[a] Mean±SD (n = 3). Solutions were diluted 1000 times for pseudo-enzymatic activity measurements. [b] Assuming Hb concentration of 1.5 mM. [c] SFHL, stroma free hemolysate. [d] Not detected.

Thermal Stability of NADH and NADPH—After aqueous solutions of NADPH and NADH dissolved in phosphate buffered saline (PBS) were sealed in vials, they were incubated at 25, 30, 37, and 50 °C. The concentration of the reduced form NAD(P)H was measured periodically by absorption at 340 nm. The initial absorbance of the NAD(P)H solutions was defined as 100% recovery. The rate constant (k) of oxidation was calculated at each incubation time. Based on those calculations, an Arrhenius plot was created (**Figure 2**). Activation energies (E_a) were calculated respectively as 251 and 167 kJ/mol for NADH and NADPH. **Table 2** presents the times necessary to reach 80 and 20% recoveries of NADH and NADPH. Apparently, NADH is more thermally stable than NADPH. For example, NADH requires 116 days to be oxidized to 20% recovery in a physiological aerobic condition, whereas NADPH requires only 1.2 days.

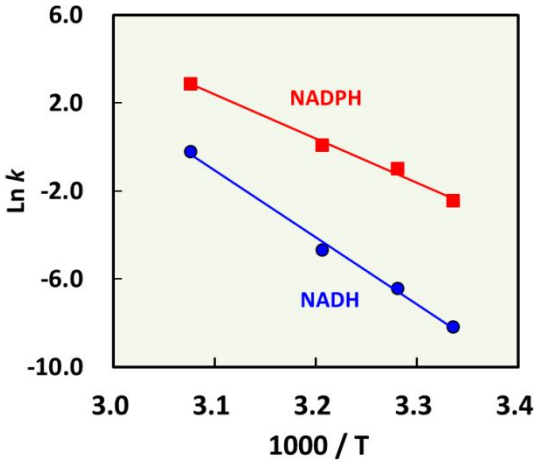

Figure 2. Arrhenius plot of rate constants (k) for the oxidation of NADH and NADPH in PBS pH 7.4 buffer.

Table 2. Oxidation of NADH and NADPH in PBS (pH 7.4, 25 or 37 °C). Symbols $t_{0.8}$ and $t_{0.2}$ respectively denote the times necessary to reach 80% and 20% recoveries.

Potential Antioxidant	$t_{0.8}$ at 25 °C (day)	$t_{0.8}$ at 37 °C (day)	$t_{0.2}$ at 37 °C (day)
NADH	834	16	116
NADPH	2.3	0.2	1.2

Michaelis Constants of the Pseudo-enzymatic Activities and Influence of IHP and DPG—Lineweaver–Burk plots (**Figure 3**) for NAD(P)H coexisting with HbO_2 were created from the data in **Table 1**. The Michaelis constants (K_m) were calculated from intersection with the X-axis. The K_m values for pseudo-CAT are 1.4 mM (NADPH) and 1.8 mM (NADH). Furthermore, those for pseudo-SOD are 2.1 mM (NADPH) and 2.3 mM (NADH). Equimolar addition of IHP or DPG to NAD(P)H coexisting with HbO_2 showed competitive inhibition patterns with consistent intersections with the Y-axis while the slope increased, indicating that the V_{max} values were consistent and that the apparent K_m increased. The inhibition dissociation constant (K_i) of IHP was higher than that for DPG. Results show that IHP inhibited the pseudo-enzymatic activities more strongly than DPG did (**Table 3**).

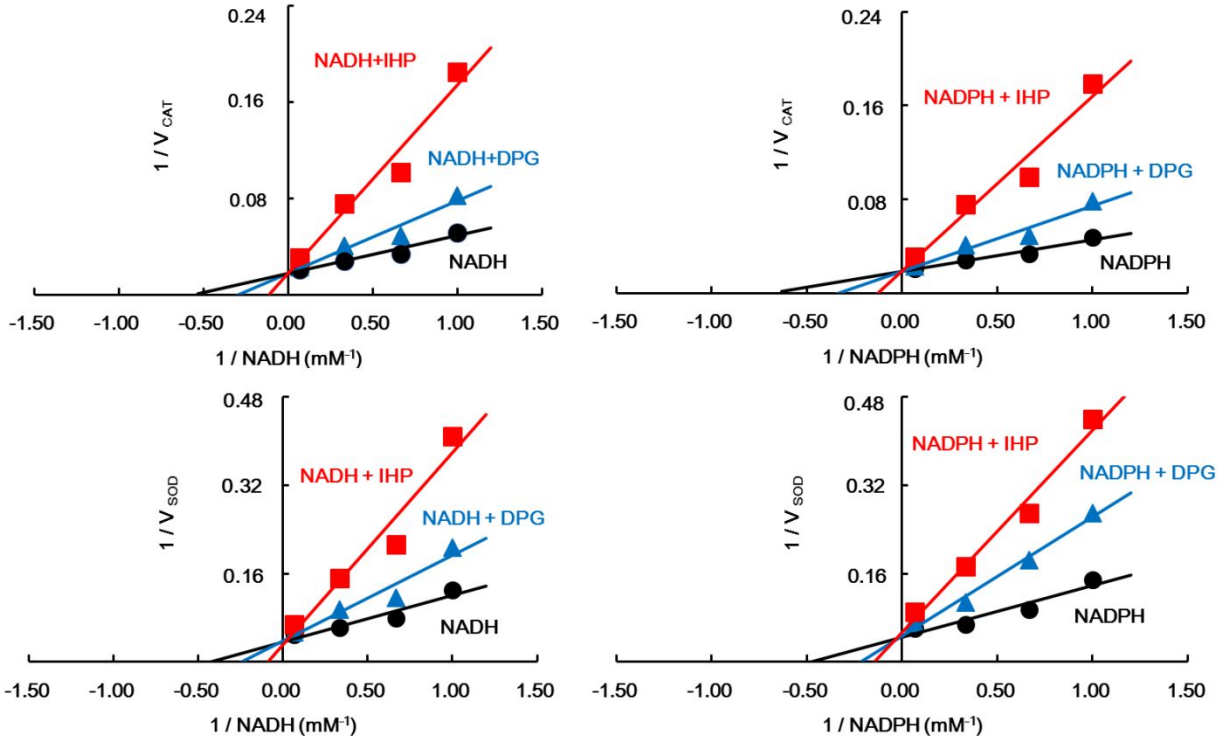

Figure 3. Lineweaver–Burk plots of pseudo-CAT and pseudo-SOD activities for NAD(P)H (1–15 mM) in the presence of 1.5 mM HbO_2, with or without equimolar IHP or DPG as inhibitors. V_{CAT}, Pseudo-CAT, $\times 10^4$ IU/g Hb; V_{SOD}, Pseudo-SOD, $\times 10^2$ U/g Hb.

***Effects of NAD(P)$^+$ and PLP on Pseudo-CAT and SOD Activities*—**Inhibitory effects of oxidized forms NAD^+ and $NADP^+$, and PLP on the pseudo-enzymatic activities of NAD(P)H coexisting with HbO_2 were examined by adding them at the equimolar concentration of NAD(P)H to create Lineweaver–Burk plots (data not shown). As a result, both V_{max} and K_m were unaffected by the addition of NAD^+, $NADP^+$, and PLP, as presented in **Table 3**.

Table 3. Kinetic parameters of the pseudo-CAT and pseudo-SOD activities of NAD(P)H with coexistence with HbO_2, and the influence of the potential inhibitors: IHP, DPG, NAD^+, $NADP^+$, and PLP.

Potential Antioxidant	Pseudo-enzymatic activity	Potential Inhibitor	K_m (mM)	V_{max} (CAT, $\times 10^4$IU/g Hb) (SOD, $\times 10^2$U/g Hb)	K_i (mM)
NADH	CAT	None	1.8	56.2	-
		IHP	8.8 [a]	56.5	2.1
		DPG	3.2 [a]	55.6	9.6
		NAD^+	2.0 [a]	56.8	-
		PLP	2.2 [a]	56.5	-
	SOD	None	2.3	27.4	-
		IHP	11.0 [a]	31.8	1.7
		DPG	4.1 [a]	26.3	8.6
		NAD^+	2.2 [a]	28.2	-
		PLP	2.1 [a]	29.0	-
NADPH	CAT	None	1.4	52.9	-
		IHP	7.8 [a]	52.4	2.4
		DPG	2.9 [a]	52.6	9.9
		$NADP^+$	1.4 [a]	54.6	-
		PLP	1.4 [a]	54.3	-
	SOD	None	2.1	22.4	-
		IHP	6.8 [a]	18.6	3.2
		DPG	4.7 [a]	21.6	5.8
		$NADP^+$	2.0 [a]	22.1	-
		PLP	1.8 [a]	21.6	-

[a] Apparent Michaelis constant in the presence of a potential inhibitor.

HPLC Analyses of the Autoxidation Intermediate Hybrids of HbO_2 in the Presence of NADH—During autoxidation of the HbO_2 solution (1.5 mM) in PBS in the absence of NADH, the chromatogram showed increases of partially oxidized intermediate hybrid signals, $\alpha_2^+\beta_2$ (elution time: 2.0 min) and $\alpha_2\beta_2^+$ (2.3 min), and then the totally oxidized $\alpha_2^+\beta_2^+$ (2.5 min) (**Figure 4A**). The ratio of the peak area of $\alpha_2^+\beta_2$ to that of $\alpha_2\beta_2^+$ was as high as 1.2 throughout the measurement, indicating that α-subunit heme is more prone to be autoxidized **(Figure 4B)**. On

the other hand, in the presence of 1.5 mM NADH, the total levels of the partially and totally oxidized Hbs were considerably suppressed as compared with those without NADH **(Figure 4A)**, and the ratio of the peak area of $\alpha_2^+\beta_2$ versus that of $\alpha_2\beta_2^+$ was lower than 0.9, indicating that NADH preferentially hindered autoxidation of α-subunit heme, presumably because NADH is located closer to α-subunit heme than to β-subunit heme.

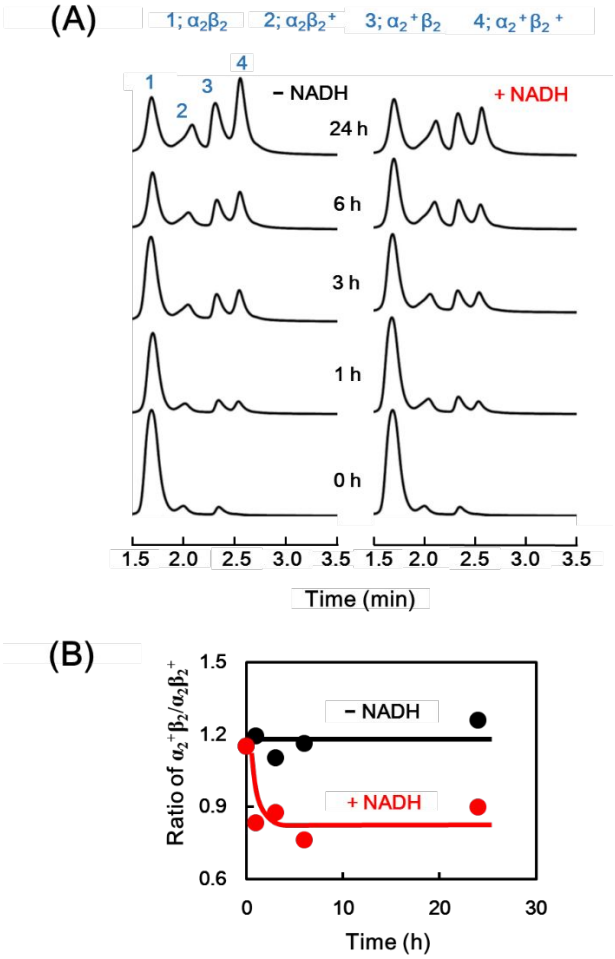

Figure 4. (A) HPLC profiles of the intermediate Hb hybrids during autoxidation of HbO_2 at 37 °C in the presence (+) and absence (-) of NADH (1.5 mM) in PBS. **(B)** Time courses of the peak area ratio of $\alpha_2^+\beta_2$ versus that of $\alpha_2\beta_2^+$, calculated from the chromatograms in (A).

^{31}P NMR of NADH in the Presence of HbO_2—NADH possesses two phosphate groups between nicotinamide and adenine but shows a singlet strong peak at around -11 ppm at the magnetic field employed, which is far different from the peak of phosphate (2.2 ppm) derived from PBS (data not shown). By the addition of HbO_2, the peak intensity decreased while other three upfield peaks appeared (**Figure 5A**). Because of the presence of irons in Hb, all the peaks tended to be left-shifted in parallel to a lower field. In the presence of equimolar amount of 1.5 mM HbO_2, the spectrum of NADH is composed of the AB quartet split pattern with J_{AB} = 20 Hz and ν_{AB} = 0.3 ppm, indicating that the two phosphate groups in the NADH molecule are located in different environments, presumably induced by the binding with HbO_2. From the integrated intensities of the signals, the percentage of the amount of NADH bound with HbO_2 was calculated for all the analytes (**Figure 5B**), considering the overlapping of the singlet signal of free NADH and the split leftmost signal of interacted NADH. The amount of NADH bound with HbO_2 proportionally increased with the amount of HbO_2. The results indicate the 1:1 stoichiometric binding of NADH to HbO_2.

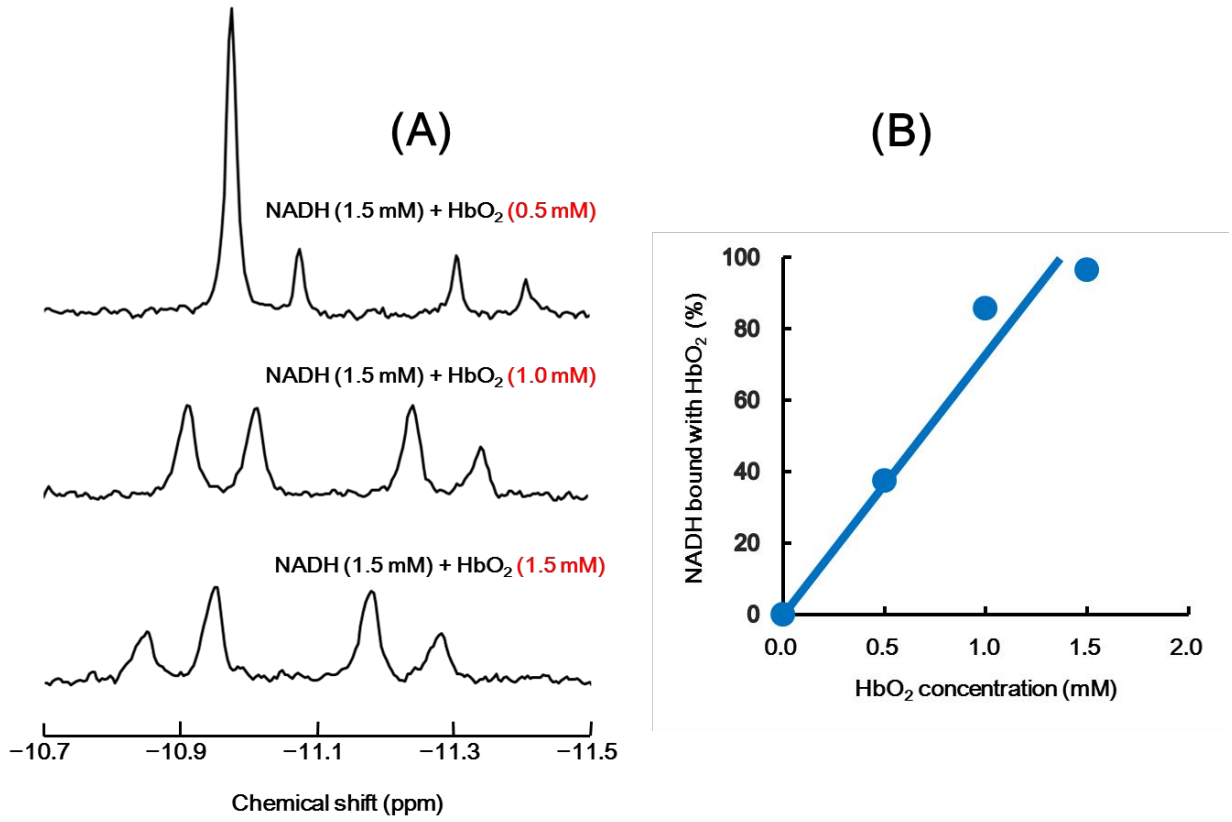

Figure 5. (A) The proton-decoupled ^{31}P NMR of NADH (1.5 mM) in the presence of HbO_2 (0.5, 1.0, and 1.5 mM) in PBS. (B) The percentage of NADH bound with HbO_2 with increaseing the amount of HbO_2.

Docking Simulation of NAD(P)H and HbO$_2$—Atomic coordinates of HbO_2 and NAD(P)H were obtained from Protein data bank (PDB) registered as X-ray structural analysis. A docking simulation was conducted using MF myPresto v3.2 mmMPApp2 application software (**Figure 6**). The interatomic distances of major sites are portrayed in **Table 4**. Reportedly, DPG binds to HbO_2 with interatomic distance of 2.57–2.89 Å between phosphate groups of DPG and α-subunit Lys99 and Arg141.[12] Our simulation clarified that both NADH and NADPH bind to the same position on HbO_2 with interatomic distance of 1.85–4.08 Å between NADH and α-subunit

Lys99 and Arg141 **(Figure 6)**, and 2.42–3.63 Å between NADPH and the same residues (see ***Supporting Information***). In **Table 4**, the set of oxygens (O8, O9) in NADH corresponds to one phosphate group near nicotinamide locating nearby α_2Lys99, and another phosphate group near nicotinamide is apparently distant from the residue. Such different environments of two phosphate groups should affect their ^{31}P NMR. The interatomic distance between the carbon (C5) in a heme and the carbon (C19) of nicotinamide is 10.08 Å for NADH **(Figure 6)** and 9.24 Å for NADPH (see ***Supporting Information***). We also simulated docking NADH to deoxyHb, which revealed that NADH binds to β-subunits, not to α-subunits, and that the distances from NADH to the β-subunit Lys82 were 2.95 Å, and to the β-subunit His143 was 3.44 Å, although the interatomic distance to the carbon (C19) of the heme structure was estimated as 19.99 Å for β1-heme (see ***Supporting Information***).

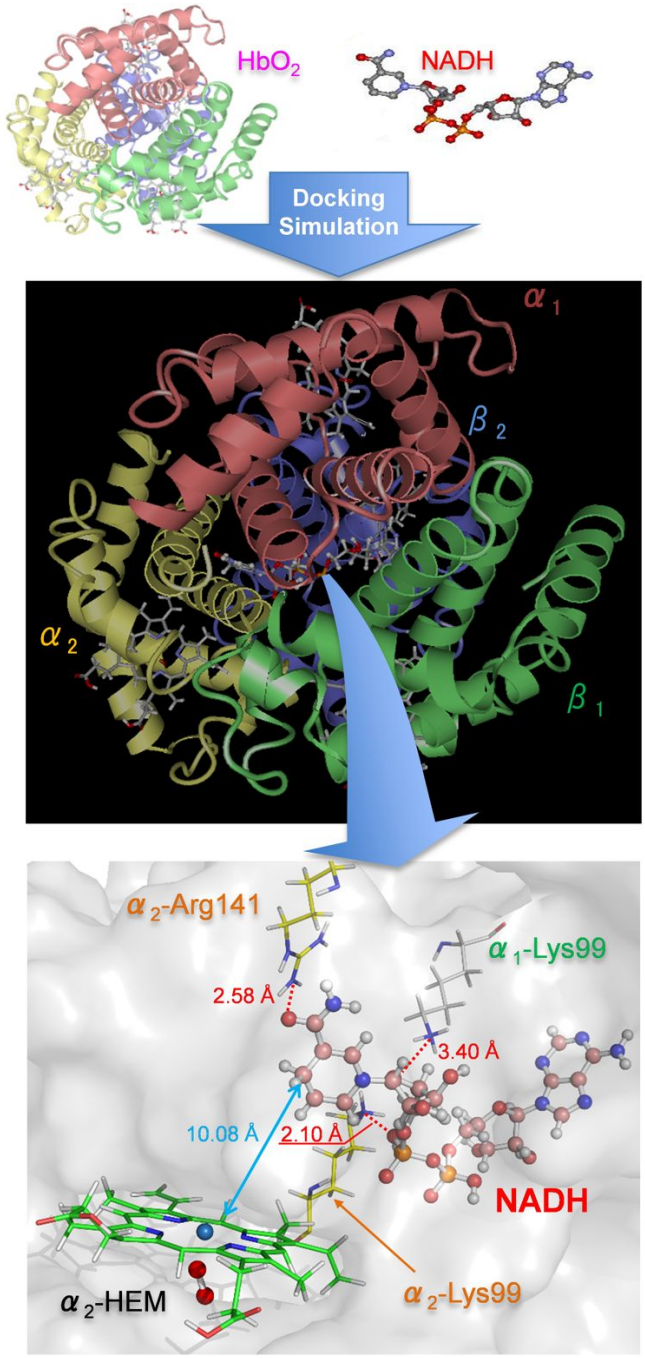

Figure 6. Proposed interacting sites between HbO_2 and NADH obtained from the docking simulation using a MF myPresto system.

Table 4. Interatomic distances (Å) between the ligand sites and protein sites (HbO_2) calculated from the docking simulation using a MF myPresto system

Ligand	Ligand-site (A)	HbO_2-site (B)	Distance (Å) between (A)–(B)
NADH	NADH-O8	α_2Lys99-NZ	3.49
	NADH-O9	α_2Lys99-NZ	2.10
	NADH-O11	α_1Lys99-NZ	3.40
	NADH-O12	α_1Lys99-NZ	4.08
	NADH-O14	α_2Arg141-NH2	1.85
	NADH-O14	α_2Arg141-NZ	2.58
	NADH-C19	**α_2HEM-C5**	**10.08**
NADPH	NADPH-O1	α_1Lys99-NZ	2.61
	NADPH-O8	α_2Lys99-NZ	3.63
	NADPH-O9	α_1Lys99-NZ	2.42
	NADPH-O10	α_2Lys99-NZ	2.83
	NADPH-O12	α_2Arg141-NZ	2.82
	NADPH-O13	α_2Arg141-NZ	3.48
	NADPH-C19	**α_2HEM-C5**	**9.24**
DPG[a]	DPG-O2	α_1Lys99-NZ	2.89
	DPG-O5	α_2Arg141-NH2	2.87
	DPG-O10	α_2Lys99-NZ	2.86
	DPG-O11	α_2Lys99-NZ	2.66
	DPG-O13	α_2Arg141-NH1	2.57
	(Wat639-O)	α_2Arg141-NH2	2.64

[a] Referred from results of an earlier study.[12]

DISCUSSION

NADH within RBCs contributes to reduction of metHb as the coenzyme of NADH-cytochrome b_5 reductase. However, our earlier report described that a high concentration of NADH coexisting with purified HbO_2 showed a reduced rate of autoxidation at 37 °C for 24 h in the absence of the corresponding enzymes.[8] An analogic molecule NADPH showed a markedly weaker effect even though both NADH and NADPH possess equal standard redox potential (E'_0 = – 0.32 V). The reason for this different effect of NADPH versus NADH was not clarified in our previous study. In the present study, we demonstrated that rapid metHb formation induced by the oxidants (H_2O_2, NO, $NaNO_2$) was suppressed by the addition of NADPH, with effects similar to those of NADH. Furthermore, the pseudo-CAT and pseudo-SOD activities of NADPH in the presence of HbO_2 were nearly equal to those of NADH. Nevertheless, a difference was found between NADH and NADPH in terms of thermal stability. For example, in an aerobic condition at 37 °C NADH requires 116 days for oxidization to 20% recovery, although NADPH requires only 1.2 days. The respective activation energies (E_a) of oxidation for NADPH and NADH are 40 and 60 kcal/mol, indicating that NADPH is very unstable. We speculate that this thermal instability is the reason that NADPH showed insufficient suppression of metHb formation over a long period of time (24 h), although both have similar pseudo-enzymatic activities in the presence of HbO_2 that are readily measurable (< 1 h).

The standard redox potential (E'_0) of both NADH and NADPH is –0.32 V. However, in some physiological conditions they show different redox potentials (E').[27,28] E' of NADH is –0.241, –0.280, or –0.318 V and that of NADPH ranges lower values; –0.370, –0.393, or –0.415 V. This difference indicates that NADPH is more prone to be oxidized. Reportedly, in an aerobic

condition NAD(P)H initially reacts with oxygen to form NAD(P)H-peroxide anion, $^{-}O_2$-NAD(P)H, which then capture a hydrogen ion to form hydrogen peroxide and oxidized $NAD(P)^+$.[26] The generated hydrogen peroxide then reacts with another NAD(P)H to form $NAD(P)^+$ and water molecule. Wu et al.[29] suggested that the different reactivity with hydrogen ion between $^{-}O_2$-NADH and $^{-}O_2$-NADPH should cause the different stability. Because ionic strength significantly affects the half-life of NADH, it is suggested that additional phosphate group present on adenosine in NADPH should influence on the local ionic strength and stabilize the oxidized pyridinyl cation of nicothinamide, that may shorten the half-life of NADPH.

Next, we analyzed the kinetic parameters of the pseudo-enzymatic activities such as the Michaelis constant (K_m). The K_m values were clarified to be of millimolar order. In the HbO_2 solution (10 g/dL, 1.55 mM), the amount of NAD(P)H necessary for the inhibition of metHb formation must be at least equimolar to HbO_2 (**Table 1**). In contrast, the K_m value of cytochrome b_5 reductase (metHb reductase system) with NADH as a coenzyme is reportedly 1.6 μM,[30] demonstrating that K_m of the NADH-HbO_2 system is about 1,000 times higher. However, co-encapsulation of such a high concentration of NADH is possible to prepare artificial red cells (liposome-encapsulated Hbs) generating the pseudo-enzymatic activities sufficient to inhibit metHb formation.[8]

The presence of two inhibitors (IHP, DPG) in the NAD(P)H-HbO_2 pseudo-enzymatic system indicated competitive inhibition because V_{max} did not change although K_m increased. X-ray structure analysis clarified that both IHP and DPG bind to the cleft of β-subunits in the tense state deoxyHb.[31,32] However, a docking simulation report described they can also interact with relaxed state HbO_2.[12,33] Therefore, it was inferred that interaction sites on HbO_2 for NAD(P)H are

the same as those for IHP and DPG.

We tried to quantify the interaction of NAD(P)H and HbO_2 using isothermal titration calorimetry, observing the generated heat by mixing two aqueous solutions. However, the heat was so low as to subtract the dilution heat for sufficient validation (data not shown). This implies that the interaction is essentially weak and their binding constants (K_b) are small. Actually, Cashon *et al.*[34] measured K_b of NADPH to HbO_2 by a subtle shift of oxygen affinity, and it was as small as 0.073 mM^{-1}. However, they failed to measure K_b of NADH, though they obtained much higher K_b for NAD(P)H to deoxyHb. Ogo *et al.*[35,36] measured K_b by fluorescence titrations of NAD(P)H and obtained K_b for deoxyHb, but not for HbO_2 because of the weak interaction. On the other hand, our data of Lineweaver-Burk plots in the presence of an equimolar inhibitor (IHP or DPG) to NAD(P)H (**Figure 3**) indicate that the inhibitor and NAD(P)H compete with each other to bind to the same site on HbO_2. Therefore, the K_b values for NAD(P)H would be presumably comparable to or lower than those of IHP (2–10 mM^{-1}) and DPG (0.4–1.2 mM^{-1}) reported in the literature.[11,12] Addition of oxidized form NAD^+ or $NADP^+$ to NAD(P)H coexisting HbO_2 showed no inhibition effect to the pseudo-enzymatic activities, indicating that neither NAD^+ nor $NADP^+$ binds to the NAD(P)H binding site. Accordingly, after the NAD(P)H-HbO_2 system shows pseudo-enzymatic activities, the oxidized $NAD(P)^+$ dissociates immediately. It is replaced with new NAD(P)H for repeated pseudo-enzymatic activity. Actually, PLP is used as an allosteric effector for Hb in liposome-encapsulated Hbs (artificial red blood cells).[8] It is known to bind to the terminals of α-chains and β-chains,[37] which is different from the binding site of NAD(P)H, explaining why PLP showed no inhibition effect.

^{31}P NMR is widely used for the analysis of weak interaction of phosphate compounds

with proteins.[38,39] ^{31}P NMR of NADH provided a direct evidence that NADH stoichiometrically interacts with HbO_2 at 1:1 molar ratio as shown in **Figure 5**. Even though NADH possesses two phosphate groups, the unbound free NADH shows a singlet signal. On the other hand, the interacted NADH showed quartet split signals, indicating that the environments of the two phosphate groups are different after binding to HbO_2. Reportedly the reason for the fact that oxidized NAD^+ shows similar quartet split signals is that the oxidized nicotinamide contains a charged nitrogen in the pyridine ring and that there is an intramolecular electrostatic interaction between this nitrogen and the negatively charged phosphate.[40] Therefore, in our study it is speculated that the phosphate groups in NADH electrostatically interacts with positive charges on the globin chain of HbO_2, inducing heterogeneous environments for the two phosphate groups. The reasons why NAD^+ does not interact with HbO_2 are that the positive charge of NAD^+ hinders the binding to the positively charged site of globin or that the molecular conformation of NAD^+ is distorted because of the intramolecular electrostatic interaction as mentioned above.

The binding site of IHP and DPG on HbO_2 is located near the α-subunit heme.[12,33] Presumably, NAD(P)H should preferentially interacts at the same site, which might be related to the antioxidative property of NAD(P)H coexisting with HbO_2 and the consequent inhibition of metHb formation. The acceleration of disproportional reaction (Eq. 1) by the pseudo-SOD activity and the elimination of ($O_2{\cdot}^-$) are expected to contribute to the reduced metHb formation reaction (Eq. 2) by H_2O_2.[8]

$$2O_2{\cdot}^- + 2H^+ \rightarrow H_2O_2 + O_2 \qquad \textbf{(Eq. 1)}$$

$$2Hb(Fe^{2+})O_2 + H_2O_2 + 2H^+ \rightarrow 2metHb(Fe^{3+}) + 2H_2O + O_2 \qquad \textbf{(Eq. 2)}$$

Regarding the mechanism of pseudo-CAT activity, the following reaction system can be considered (Eqs. 3 and 4). First, metHb reacts to H_2O_2, generating ferryl Hb radical (Fe^{4+}=O),

which in turn interacts with NADH, providing it with two electrons. Then H_2O_2 is eliminated while metHb is reproduced.[41]

$$\text{H-metHb}(Fe^{3+}) + H_2O_2 \rightarrow \cdot\text{ferrylHb}(Fe^{4+}{=}O) + H_2O + H^+ \quad \textbf{(Eq. 3)}$$

$$\cdot\text{ferrylHb}(Fe^{4+}{=}O) + NADH + 2H^+ \rightarrow \text{H-metHb}(Fe^{3+}) + NAD^+ + H_2O \quad \textbf{(Eq. 4)}$$

We have been trying crystallization of HbO_2 in the presence of NADH for the detailed structural analysis by X-ray crystallography. However, it is not successful so far probably because of the very weak interaction between NADH and HbO_2. Laberge *et al.*,[12] conducted structural analysis using docking simulation on phosphate compounds such as 2,3-DPG and IHP which are weakly bound to the relax state HbO_2. Therefore, we have no choice but to test docking simulation. Our docking simulation of NADH and HbO_2 estimated the binding sites of NADH on HbO_2. The interatomic distance of DPG (phosphate group) and HbO_2 (α-subunit Lys99, Arg141), obtained with docking simulation by Laberge *et al.*, is reportedly 2.57–2.89 Å.[12] As shown in **Figure 6**, the interatomic distance of NADH and the amino acid residues of HbO_2 was 1.85–4.08 Å, which surely allows potential binding. The interatomic distance between the carbon (C5) in α-subunit heme skeleton and the carbon (C19) of nicotinamide site relating to the redox was 10.08 Å. This is a long distance, but it has been presented in some reports of the literature[42-44] that electron transfer is possible even at 10.5 Å in perturbing proteins, supporting the potential electron transfer from NADH to a heme over this interatomic distance. In addition, the interatomic distance between NADPH and the amino acid residues of HbO_2 was estimated as 2.42–3.63 Å. That of a heme and nicotinamide is 9.24 Å. These interatomic distances of NADPH are equivalent to those of NADH. When oxidizing substances such as ROS approach a heme iron, the oxidation of heme can be inhibited by the reducing power of adjacent NAD(P)H bound to HbO_2. Actually, ROS is expected to be eliminated by pseudo-SOD and pseudo-CAT; metHb

formation was inhibited by this effect.

Because the binding site of NAD(P)H on HbO_2 seems preferentially in α-subunits and not in β-subunits, it is expected that the oxidation of β-subunit heme would be less inhibited. Actually, HPLC profiles of the metHb intermediates during autoxidation showed relatively higher degree of inhibitory effect of NADH on α-subunit heme as shown in **Figure 4**, supporting that NADH locates near the α-subunit heme.

The docking simulation of deoxyHb and NADH clarified that the binding residues are β-subunit Lys82 and His143 with interatomic distances of 2.95 and 3.44 Å, respectively (see ***Supporting Information***). In addition, the K_b value for deoxyHb is presumably higher than that for HbO_2.[34-36] However, the interatomic distance between heme and NADH is as long as 20 Å; this distance would allow electron transfer between them only to a slight degree. The measurement of pseudo-enzymatic activities cannot be done in a deoxygenated condition because of the generation of dioxygen in the analyte solution. However, it is speculated that the pseudo-enzymatic activities of NAD(P)H coexisting with deoxyHb are low in comparison to those of HbO_2.

Intraerythrocytic concentrations of NAD^+ and NADH are 6.5×10^{-2} mM and 2.8×10^{-4} mM, respectively.[9] Those of $NADP^+$ and NADH are 6.5×10^{-5} mM and 6.5×10^{-2} mM, respectively. The amount of NAD(P)H bound to Hb (5.4 mM) should be very small. The physiological role of the pseudo-enzymatic activities of the combination of NAD(P)H-HbO_2 in a normal healthy condition is not known, however, it would be conceivable that such antioxidative function works in a genetic disease such as deficiency of ROS-eliminating enzymatic systems.

One limitation of this antioxidative system is that it does not completely eliminate metHb formation and requires the corresponding metHb reducing enzymatic system to maintain a lower level of metHb formation. However, it should be emphasized that co-encapsulation of NADH in artificial red blood cells (liposome-encapsulated Hbs: Hb-vesicles) at 1:1 ratio, that do not contain any corresponding enzymes, show retarded metHb formation in blood circulation as shown in the previous report[8]. This prolongs the functional life span of artificial red cells in blood circulation for a clinical use.

CONCLUSION

Results of this study clarified the mechanism of the antioxidative properties induced by the interaction of NAD(P)H and HbO_2. The formation of metHb was inhibited by NAD(P)H at a high concentration coexisting with HbO_2. The interaction between NAD(P)H and HbO_2 is so weak and the crystallinity of HbO_2 is so low in the physiological condition that we have not obtained a co-crystal for X-ray crystallography. Therefore, we estimated the binding site of NAD(P)H on HbO_2 from various perspectives, such as competitive inhibition of pseudo-enzymatic activities in the presence of IHP and DPG of which the binding sites are already known, the dominant antioxidative effect on α subunit, stoichiometric binding of NADH to Hb clarified by ^{31}P NMR, and the docking simulation that predicted the nicotinamide of NAD(P)H as a redox center can be located in the vicinity of α subunit heme, where ROS can be eliminated by pseudo-enzyme activities.

ASSOCIATED CONTENT

Supporting Information

Docking simulations were conducted for HbO_2 with NADPH and deoxyHb with NADH. The data are listed as *Supporting Information*.

AUTHOR INFORMATION

Corresponding Author

*Prof. Hiromi Sakai. Tel. and Fax: +81-(0)744-29-8810. E-mail: hirosakai@naramed-u.ac.jp.

ORCID

Takashi Matsuhira: 0000-0003-2429-9847

Hiromi Sakai: 0000-0002-0681-3032

Author Contributions

The manuscript was composed based on the contributions of all authors. All authors have given approval to publication of the final version of the manuscript.

Notes

The authors declare the following competing financial interest: Authors M.Y. and H.S. are inventors holding some patents related to the production and utilization of Hb-vesicles.

ACKNOWLEDGMENTS

We acknowledge Prof. Akiyoshi Tanaka and Dr. Hideo Miyake (Graduate School of Bioresources, Mie University) for their advice related to thermal analysis. This research was supported by Grants-in Aid for Scientific Research (Kiban B, 25282136 and 17H02087) from the Japan Society for the Promotion of Sciences (JSPS).

REFERENCES

1. Tsuruga, M., Matsuoka, A., Hachimori, A., Sugawara, Y., and Shikama, K. (1998) The molecular of mechanism of autoxidation for human oxyhemoglobin Tilting of the distal histidine causes nonequivalent oxidation in the beta chain. *J. Biol. Chem*. 273, 8607−8615.
2. Winterbourn, C.C., McGrath, B.M., and Carrell, R.W. (1976) Reactions involving superoxide and normal and unstable haemoglobins. *Biochem. J.* 155, 493–502.
3. Marklund, S., and Marlund, G. (1974) Involvement of the superoxide anion radical in the autooxidation of pyrogallol and a convenient assay for superoxide dismutase. *Eur. J. Biochem*. 47, 469–474.
4. Hamon, I., Gauthier-Moulinier, H., Grelet-Dessioux, E., Storme, L., Fresson, J., and Hascoet, J. M. (2010) Methaemoglobinaemia risk factors with inhaled nitric oxide therapy in newborn infants. *Acta Paediatr*. 99, 1467−1473.
5. Kuma, F. (1981) Properties of methemoglobin reductase and kinetic study of methemoglobin reduction. *J. Biol. Chem.* 256*,* 5518–5523.

6. Kinoshita, A., Nakayama, Y., Kitayama, T., and Tomita, M. (2007) Simulation study of methemoglobin reduction in erythrocytes. Differential contributions of two pathways to tolerance to oxidative stress. *FEBS J*. 274, 1449−1458.

7. Stanton, R.C. (2012) Critical review. Glucose-6- phosphate dehydrogenase, NADPH, and cell survival. *IUBMB Life* 64, 362–369.

8. Yamada, M., and Sakai, H. (2017) Hidden antioxidative functions of reduced nicotinamide adenine dinucleotide coexisting with hemoglobin. *ACS Chem. Biol.* 12, 1820–1829.

9. Kinoshita, A., Tsukada, K., Soga, T., Hishiki, T., Ueno, Y., Nakayama, Y., Tomita, M., and Suematsu, M.（2007）Roles of hemoglobin allostery in hypoxia-induced metabolic alterations in erythrocytes: simulation and its verification by metabolome analysis. *J. Biol. Chem.* 282, 10731–10741.

10. Birkmayer, J.G., Nadlinger, K.F., and Hallström, S. (2004) On the safety of reduced nicotinamide adenine dinucleotide (NADH). *J. Environ. Pathol. Toxicol. Oncol*. 23, 179–194.

11. Imaizumi, K., Imai, K., and Tyuma, I. (1979) The linkage between the four-step binding of oxygen and the binding of heterotropic anionic ligands in hemoglobin. *J. Biochem*. 86, 1829–1840.

12. Laberge, M., Kövesi, I. Yonetani, T., and Fidy, J. (2005) R-state hemoglobin bound to heterotropic effectors: models of the DPG, IHP and RSR13 binding sites. *FEBS Lett.* 579, 627–632.

13. Sakai, H., Masada, Y., Takeoka, S., and Tsuchida, E. (2002) Characteristics of bovine hemoglobin as a potential source of hemoglobin-vesicles for an artificial oxygen carrier. *J. Biochem.* 131, 611–617.

14. Sakai, H., Takeoka, S., Yokohama, H., Seino, Y., Nishide, H., and Tsuchida, E. (1993) Purification of concentrated hemoglobin using organic solvent and heat treatment. *Protein*

Expr. Purif. 4, 563–569.

15. Di Iorio, E. E. (1981) Preparation of methemoglobin. *Methods Enzymol.* 76, 65–66.
16. Chance, B. (1954) Catalases and peroxidases, part II. Special methods. *Methods Biochem. Anal.* 1, 408–424.
17. Marklund, S., and Marklund, G. (1974) Involvement of the superoxide anion radical in the autoxidation of pyrogallol and a convenient assay for superoxide dismutase. *Eur. J. Biochem.* 47, 469–474.
18. Roth, E. F. Jr., and Gilbert, H. S. (1984) The pyrogallol assay for superoxide dismutase: absence of a glutathione artifact. *Anal. Biochem.* 137, 50–53.
19. Xin, L., Ipek, Ö., Beaumont, M., Shevlyakova, M., Christinat, N., Masoodi, M., Greenberg, N., Gruetter, R., and Cuenoud, B. (2018) Nutritional ketosis increases NAD^+/NADH ratio in healthy human brain: An *in vivo* study by ^{31}P-MRS. *Front. Nutr.* 5, 62.
20. Lu, M., Zhu, X.H., and Chen W. (2016) In vivo ^{31}P MRS assessment of intracellular NAD metabolites and NAD^+/NADH redox state in human brain at 4 T. *NMR Biomed.* 29, 1010–1017.
21. Blumenstein, M., and Raftery, M. A. (1972) ^{31}P and ^{13}C nuclear magnetic studies of nicotinamide-adenine dinucleotide and related compounds. *Biochemistry* 11, 1643–1648.
22. Shaanan, B. (1983) Structure of human oxyhaemoglobin at 2.1 Å resolution. *J. Mol. Biol*. 171, 31–59.
23. Fermi, G., Perutz, M.F., Shaanan, B. and Fourme, R. (1984) The crystal structure of human deoxyhaemoglobin at 1.74 Å resolution. *J. Mol. Biol*. 175, 159–174.
24. Meijers, R., Adolph, H.W., Dauter, Z., Wilson, K.S., Lamzin, V.S. and Cedergren-Zeppezauer, E.S. (2007) Structural evidence for a ligand coordination switch in liver alcohol dehydrogenase. *Biochemistry* 46, 5446–5454.

25. Howard, E.I., Sanishvili, R., Cachau, R.E., Mitschler, A., Chevrier, B., Barth, P., Lamour, V., Van Zandt, M., Sibley, E., Bon, C., Moras, D., Schneider, T.R., Joachimiak, A. and Podjarny, A. (2004) Ultrahigh resolution drug design I: details of interaction in human aldose reductase-inhibitor complex at 0.66 Å. *Proteins* 55, 792–804.

26. Bernofsky, C., and Wanda, Y. C. (1982) Formation of reduced nicotinamide adenine dinucleotide peroxide. *J. Biol. Chem.* 257, 6809−6817.

27. Huang, H., Wang, S., Moll, J., and Thauer, R.K. (2012) Electron bifurcation involved in the energy metabolism of the acetogenic bacterium *Moorella thermoacetica* growing on glucose or H_2 plus CO_2. *J. Bacteriol.* 194, 3689–3699.

28. Jones, D.P., and Sies, H. (2015) The redox code. *Antioxid. Redox Signal.* 23, 734–746.

29. Wu, J. T., Wu, L. H., and Knight, J. A. (1986) Stability of NADPH: effect of various on the kinetics of degradation. *Clin. Chem.* 32, 314−319.

30. Passon, P.G., and Hultquist, D.E. (1972) Soluble cytochrome b_5 reductase from human erythrocytes. *Biochim. Biophys. Acta* 275, 62–73.

31. Luisi, B., Liddington, B., Fermi, G., and Shibayama, N. (1990) Structure of deoxy – quaternary haemoglobin with ligated beta subunits. *J. Mol. Biol.* 214, 7–14.

32. Bonaventura, J., Bonaventura, C., Sullivan, B., and Godette, G. (1975) Hemoglobin Deer Lodge (β2 His→Arg) consequences of altering the 2,3-diphosphoglycerate binding site *J. Biol. Chem*. 250, 9250–9255.

33. Song, X. J., Simplaceanu, V., Ho, N. T., and Ho, C. (2008) Effector –induced structural fluctuation regulates the ligand affinity of an allosteric protein: binding of inositol hexaphosphate has distinct dynamic consequences for the T and R states of hemoglobin. *Biochemistry* 47, 4907–4915.

34. Cashon, R., Bonaventura, C., Bonaventura, J., and Focesi, A. (1986) The nicotinamide

adenine dinucleotides as allosteric effectors of human hemoglobin. *J. Biol. Chem*. 261, 12700–12705.

35. Ogo, S., Focesi, A. Jr., Cashon, R., Bonaventura, J., and Bonaventura, C. (1989) Interaction of nicotinamide adenine di nucleotides with varied states and forms of hemoglobin. *J. Biol. Chem*. 264, 11302–11306.

36. Ogo, S.H., Focesi A. Jr., Cashon, R., Bonaventura, C., and Bonaventura, J. (1987) Fluorescence studies of the binding of reduced nicotinamide adenine dinucleotide phosphate to human hemoglobin A and its variant hemoglobin providence. *Braz. J. Med. Biol. Res.* 20, 755–758.

37. Schnackerz, K.D., Benesch, R.E., Kwong, S., Benesch, R., and Helmreich, E. J. (1983) Specific receptor sites for pyridoxal 5'-phosphate and pyridoxal 5'-deoxymethylenephosphonate at the α and β NH_2-terminal regions of hemoglobin. *J. Biol. Chem*. 258, 872–875.

38. Marta, M., Patamia, M., Colella, A., Sacchi, S., Pomponi, M., Kovacs, K.M., Lydersen, C., and Giardina, B. (1998) Anionic binding site and 2,3-DPG effect in bovine hemoglobin. *Biochemistry* 37, 14024–14029.

39. Eyschen, J., Vitoux, B., Rahuel-Clermont, S., Marraud, M., Branlant, G., and Cung, M.T. (1996) Phosphorus-31 nuclear magnetic resonance studies on coenzyme binding and specificity in glyceraldehyde-3-phosphate dehydrogenase. *Biochemistry* 35, 6064–6072.

40. Tomoda, A., Tsuji, A., and Yoneyama, Y. (1980) Mechanism of hemoglobin oxidation by ferricytochrome c under aerobic and anaerobic conditions. *J. Biol. Chem.* 255, 7978–7983.

41. Masuoka, N., Kodama, H., Abe, T., Wang, D. H., and Nakano, T. (2003) Characterization of hydrogen peroxide removal reaction by hemoglobin in the presence of reduced pyridine nucleotides. *Biochim. Biophys. Acta, Mol. Basis Dis*. 1637, 46−54.

42. Moser, C.C., Keske, J.M., Warncke, K., Farid, R.S., and Dutton, P. L. (1992) Nature of biological electron transfer. *Nature* 355, 796–802.

43. Onuchic, J.N., Beratan, D.N., Winkler, J.R., and Gray, H.B. (1992) Pathway analysis of protein electron-transfer reactions. *Ann. Rev. Biophys. Biomol. Struct.* 21, 349–377.

44. Moser, C.C., Page, C.C., Chen, X., and Dutton, P.L. (2000) Electron transfer in natural proteins theory and design. *Subcell. Biochem.* 35, 1–28.

Accession IDs for Proteins Reported in This Study

In this study human adult hemoglobin (Hb) was purified from human red blood cells. One Hb is consisted of two alpha subunits and two beta subunits. UniProtKB entry P69905 is for hemoglobin subunit alpha, and entry P68871 is for beta.

Graphic for the table of contents